Three-band $s\pm$ Eliashberg theory and the superconducting gaps of iron pnictides

G. A. Ummarino,* M. Tortello, D. Daghero, and R. S. Gonnelli
Dipartimento di Fisica and CNISM, Politecnico di Torino, Corso Duca degli Abruzzi 24, 10129 Torino, Italy
(Received 10 April 2009; revised manuscript received 7 October 2009; published 11 November 2009)

Superconductivity in iron pnictides has been recently proposed to be due to spin-fluctuation mediated coupling between hole and electron bands with order parameters of opposite sign. BCS multiband models give qualitative predictions but cannot simultaneously reproduce the experimental values of critical temperature and energy gaps. We show, instead, that a three-band strong-coupling Eliashberg model can quantitatively reproduce the gaps and their temperature dependence in both the 1111 and 122 families. We also show that this requires small typical boson energies (in agreement with experiments) and high values of the electron-boson coupling constants.

DOI: 10.1103/PhysRevB.80.172503 PACS number(s): 74.70.Dd, 74.20.Fg, 74.20.Mn

The recently discovered Fe-based pnictide superconductors[1–3] have aroused great interest in the scientific community. They have indeed shown that high-T_c superconductivity does not uniquely belong to cuprates but can take place in Cu-free systems as well. As in cuprates, superconductivity occurs upon charge doping of a magnetic parent compound above a certain critical value. However, important differences exist: the parent compound in cuprates is a Mott insulator with localized charge carriers and a strong Coulomb repulsion between electrons; in the pnictides, instead, it is a bad metal and shows a tetragonal to orthorhombic structural transition below ≈ 140 K, followed by an antiferromagnetic (AF) spin-density-wave order.[4] Charge doping gives rise to superconductivity and, at the same time, inhibits the occurrence of both the static magnetic order and the structural transition. The Fermi surface consists of two or three holelike sheets around Γ point of the reduced Brillouin zone and two electronlike sheets around M point. Up to now, the most intensively studied systems are the 1111 compounds, $ReFeAsO_{1-x}F_x$(Re=La,Sm,Nd,Pr, etc.) and especially the 122 ones, hole- or electron-doped AFe_2As_2(A=Ba,Sr,Ca). The huge amount of experimental work already done in 122 compounds is due to the availability of rather big high-quality single crystals.

Most of the present research effort is spent clarifying the microscopic pairing mechanism responsible for superconductivity. The conventional phonon-mediated coupling mechanism cannot explain the observed high T_c within standard Migdal-Eliashberg theory and the inclusion of multiband effects increases T_c only marginally.[5] On the other hand, the magnetic nature of the parent compound seems to favor a magnetic origin of superconductivity and a coupling mechanism based on nesting-related AF spin fluctuations (SF) has been proposed.[6] It predicts an interband sign reversal of the order parameter between different sheets of the Fermi surface ($s\pm$ symmetry). The number, amplitude, and symmetry of the superconducting energy gaps are indeed fundamental physical quantities that any microscopic model of superconductivity has to account for. Experiments with powerful techniques such as angle-resolved photoemission spectroscopy (ARPES), point-contact spectroscopy, scanning tunnel microscopy (STM), etc., have been carried out to study the superconducting gaps in pnictides (for a review see Ref. 7). Although results are sometimes in disagreement with each other, a multigap scenario is emerging with evidence for rather high gap ratios, $\Delta_1/\Delta_2 \approx 2-3$.[7] A two-band BCS model cannot account either for the amplitude of the experimental gaps and for their ratio. Three-band BCS models have been investigated[8–10] which can reproduce the experimental gap ratio but not the exact experimental gap values. In this regard a reliable study has to be carried out within the framework of the Eliashberg theory for strong-coupling superconductors,[11] due to the possible high values of the coupling constants necessary to explain the experimental data.

By using this strong-coupling approach, we show here that the proposed interband only, $s\pm$-wave model can indeed describe superconductivity in pnictides, but only if high values of the electron-boson coupling constants and small typical boson energies are used. Furthermore we prove that a small contribution of intraband coupling does not affect significantly the obtained results. The model is compared with the results of two representative experiments in 122 (Ref. 12) and 1111 (Ref. 13) compounds, proving to be able to reproduce fairly well the values and the whole temperature dependence of the energy gaps.

As a starting point, we can model the electronic structure of pnictides by using a three-band model (Fig. 1) with two hole bands (1 and 2) and one equivalent electron band (3).[9] The s-wave order parameters of the hole bands have opposite sign with respect to that of the electron one.[6] Intraband coupling could be provided by phonons while interband coupling by antiferromagnetic spin fluctuations. In a one-band system, SF are always pair breaking but in a multiband one the interband term can contribute to increase the critical temperature. Indeed, in the multiband Eliashberg equations (EE) the SF term in the intraband channel has positive sign for the renormalization functions Z_i and negative sign for the superconducting order parameters Δ_i thus leading to a strong reduction in T_c. However, if we consider negative *interband* contributions in the Δ_i equations, the final result can be an increase in the critical temperature.[14]

Let us consider the generalization of the Eliashberg theory[11] for multiband systems, that has already been used with success to study MgB_2.[15] To obtain the gaps and the critical temperature within the s-wave, three-band Eliashberg equations one has to solve six coupled integral equations for the gaps $\Delta_i(i\omega_n)$ and the renormalization functions $Z_i(i\omega_n)$, where i is a band index that ranges between 1 and 3 (see Fig. 1) and ω_n are the Matsubara frequencies. For completeness

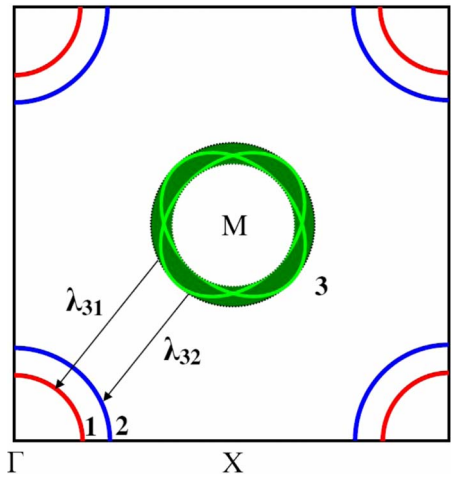

FIG. 1. (Color online) Schematic drawing of the multiband model used in this work. The two hole bands (1 and 2) are centered around the Γ point while the equivalent electron band (3) around the *M* point of the reduced Brillouin zone.

we included in the equations the nonmagnetic and magnetic impurity-scattering rates in the Born approximation, Γ_{ij}^{N} and Γ_{ij}^{M},

$$\omega_n Z_i(i\omega_n) = \omega_n + \sum_j (\Gamma_{ij}^N + \Gamma_{ij}^M) N_j^Z(i\omega_n) + \pi T \sum_{m,j} \Lambda_{ij}^Z(i\omega_n - i\omega_m) N_j^Z(i\omega_m), \quad (1)$$

$$Z_i(i\omega_n)\Delta_i(i\omega_n) = \sum_j (\Gamma_{ij}^N - \Gamma_{ij}^M) N_j^\Delta(i\omega_n) + \pi T \sum_{m,j} [\Lambda_{ij}^\Delta(i\omega_n - i\omega_m) - \mu_{ij}^*(\omega_c)] \times \theta(\omega_c - |\omega_m|) N_j^\Delta(i\omega_m), \quad (2)$$

where $\Lambda_{ij}^Z(i\omega_n - i\omega_m) = \Lambda_{ij}^{ph}(i\omega_n - i\omega_m) + \Lambda_{ij}^{sp}(i\omega_n - i\omega_m)$ and $\Lambda_{ij}^\Delta(i\omega_n - i\omega_m) = \Lambda_{ij}^{ph}(i\omega_n - i\omega_m) - \Lambda_{ij}^{sp}(i\omega_n - i\omega_m)$. θ is the Heaviside function and ω_c is a cutoff energy. In particular, $\Lambda_{ij}^{ph,sp}(i\omega_n - i\omega_m) = \int_0^{+\infty} 2\Omega d\Omega \alpha_{ij}^2 F^{ph,sp}(\Omega) / [(\omega_n - \omega_m)^2 + \Omega^2]$, where *ph* means "phonon;" and *sp* "spin fluctuations." Finally,

$$N_j^\Delta(i\omega_m) = \Delta_j(i\omega_m)/\sqrt{\omega_m^2 + \Delta_j^2(i\omega_m)}$$

and

$$N_j^Z(i\omega_m) = \omega_m/\sqrt{\omega_m^2 + \Delta_j^2(i\omega_m)}.$$

In principle, the solution of the three-band EE shown in Eqs. (1) and (2) requires a huge number of input parameters: (i) nine electron-phonon spectral functions, $\alpha_{ij}^2 F^{ph}(\Omega)$; (ii) nine electron-SF spectral functions, $\alpha_{ij}^2 F^{sp}(\Omega)$; (iii) nine elements of the Coulomb pseudopotential matrix, $\mu_{ij}^*(\omega_c)$; and (iv) nine nonmagnetic (Γ_{ij}^N) and nine paramagnetic (Γ_{ij}^M) impurity-scattering rates.

It is obvious that a practical solution of these equations requires a drastic reduction in the number of free parameters of the model. On the other hand, from the work of Mazin *et al.*[9] we know that: (i) $\lambda_{ii}^{ph} \gg \lambda_{ij}^{ph} \approx 0$, i.e., phonons mainly provide intraband coupling but the total electron-phonon coupling constant $\Sigma_i \lambda_{ii}^{ph}$ should be very small,[5] (ii) $\lambda_{ij}^{sp} \gg \lambda_{ii}^{sp} \approx 0$, i.e., SF mainly provide interband coupling. We include these features in the simplest three-band model by posing: $\lambda_{ii}^{ph} = \lambda_{ij}^{ph} = 0$, $\lambda_{ii}^{sp} = 0$, and $\mu_{ii}^*(\omega_c) = \mu_{ij}^*(\omega_c) = 0$. In addition, we set $\Gamma_{ij}^N = \Gamma_{ij}^M = 0$ in Eqs. (1) and (2).

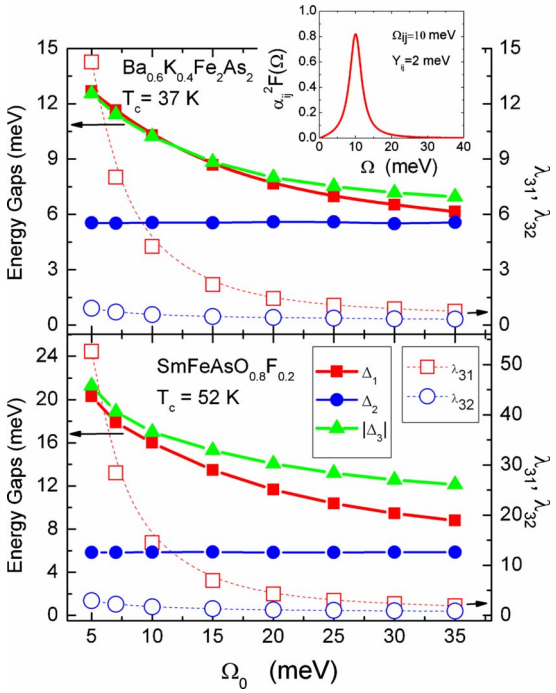

FIG. 2. (Color online) Full symbols, left axis: calculated gap values at $T=2$ K for $Ba_{0.6}K_{0.4}Fe_2As_2$ (upper panel) and $SmFeAsO_{0.8}F_{0.2}$ (lower panel) as function of typical boson energy Ω_0. Open symbols, right axis: electron-boson coupling constants, λ_{31} and λ_{32} vs Ω_0. Inset: an example of spectral function used in this model in the case $\Omega_{ij}=10$ meV.

Under these approximations, the electron-boson coupling-constant matrix is then[9]

$$\begin{pmatrix} 0 & 0 & \lambda_{31}\nu_1 \\ 0 & 0 & \lambda_{32}\nu_2 \\ \lambda_{31} & \lambda_{32} & 0 \end{pmatrix},$$

where $\nu_1 = N_1(0)/N_3(0)$, $\nu_2 = N_2(0)/N_3(0)$, and $N_i(0)$ is the normal density of states at the Fermi level for the *i*th band ($i=1,2,3$ according to Fig. 1).

The solution of the imaginary-axis EE [Eqs. (1) and (2)] can give the critical temperature and, once analytically continued to the real axis, the low-temperature values of the gaps $\Delta_i(i\omega_{n=0})$. However, in the presence of a strong-coupling interaction or impurities, these values can be very different from the values of Δ_i obtained by directly solving the real-axis EE.[16] Therefore, to determine the exact temperature dependence of the gaps we solved the three-band EE in the real-axis formulation.

We tried to reproduce the critical temperature and the gap values in two representative cases: (i) the 122 compound $Ba_{0.6}K_{0.4}Fe_2As_2$ with $T_c=37$ K where ARPES measurements gave $\Delta_1(0) \approx 12.1$ meV, $\Delta_2(0) \approx 5.5$ meV, and $\Delta_3(0) \approx 12.8$ meV;[12] (ii) the 1111 compound

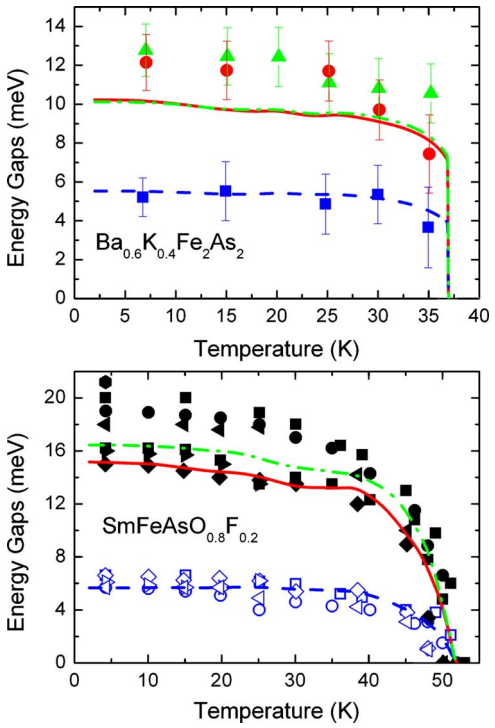

FIG. 3. (Color online) Calculated temperature dependence of the gaps for $Ba_{0.6}K_{0.4}Fe_2As_2$ (T_c=37 K, upper panel) and for $SmFeAsO_{0.8}F_{0.2}$ (T_c=52 K, lower panel): $\Delta_1(T)$ (solid line), $\Delta_2(T)$ (dashed line), and $\Delta_3(T)$ (dash-dot line). Symbols are experimental data from Ref. 12 (upper panel) and Ref. 13 (lower panel).

$SmFeAsO_{0.8}F_{0.2}$ with T_c=52 K where from point-contact spectroscopy measurements we obtained $\Delta_1(0)=18\pm3$ meV and $\Delta_2(0)=6.15\pm0.45$ meV.[13]

Inelastic neutron-scattering experiments suggest that the typical boson energy possibly responsible for superconductivity ranges roughly between 10 and 30 meV.[17] In our numerical simulations we used spectral functions $\alpha^2_{ij}F(\Omega)$ with Lorentzian shape (see the inset to Fig. 2) suitably normalized to obtain the proper values of λ_{ij}. This choice is not crucial since it can be shown that, as a first approximation, the solutions do not depend on the shape of $\alpha^2_{ij}F(\Omega)$ but only on its representative frequency.[15,18] Let Ω_{ij} and Y_{ij} be the peak energy of our Lorentzian curves and their half width, respectively. In all our calculations we set $\Omega_{ij}=\Omega_0$, with Ω_0 ranging between 5 and 35 meV, and Y_{ij}=2 meV. The cutoff energy is $\omega_c=12\Omega_0$ and the maximum quasiparticle energy is $\omega_{max}=16\Omega_0$.

In the 122 case (T_c=37 K) we know that $\nu_1=1$ and $\nu_2=2$ (Ref. 9) while in the 1111 case (T_c=52 K) we have $\nu_1=0.4$ and $\nu_2=0.5$.[19] Once the energy of the boson peak, Ω_0 is set, only two free parameters are left in the model: λ_{31} and λ_{32}.

By properly selecting the values of these parameters it is relatively easy to obtain the experimental values of the critical temperature and of the small gap. It is more difficult to reproduce the values of the large gaps of band 1 and 3 since, due to the high $2\Delta_{1,3}/k_BT_c$ ratio (on the order of 8–9), high values of the coupling constants and small boson energies are required. Figure 2 shows the values of the calculated

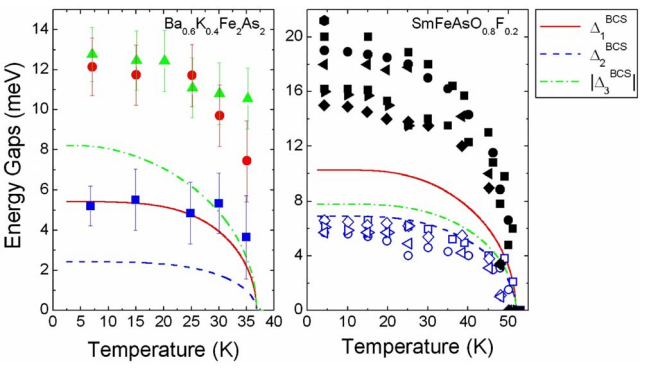

FIG. 4. (Color online) Comparison of the experimental data shown in Fig. 3 to the temperature dependence of the gaps calculated in the weak-coupling three-band BCS limit.

gaps (full symbols, left axis) as a function of the boson peak energy, Ω_0. The corresponding values of λ_{31} and λ_{32}, chosen in order to reproduce the values of T_c and of the small gap, Δ_2, are also shown in the figure (open symbols, right axis). In both materials, the value of the large gaps correspond to the experimental data only when $\Omega_0 \leq 10$ meV. Indeed, when Ω_0 increases, the values of Δ_1 and Δ_3 strongly decrease. As a consequence, a rather small energy of the boson peak together with a very strong coupling (particularly in the 3–1 channel) is needed to simultaneously obtain the experimental T_c and the correct gap values.

Another important result of the model is the temperature dependence of the gaps. Figure 3 shows this dependence for the experimental gaps (symbols) together with the theoretical $\Delta_i(T)$ curves obtained by the three-band Eliashberg model (lines) for $Ba_{0.6}K_{0.4}Fe_2As_2$ (upper panel) and $SmFeAsO_{0.8}F_{0.2}$ (lower panel). The parameters used for the 122 compound are Ω_0=10 meV, λ_{31}=4.267, and λ_{32}=0.569; for the 1111 compound we used Ω_0=10 meV, λ_{31}=14.520, and λ_{32}=1.708. Incidentally, note that with these parameters $\lambda_{ij}\Omega_0 \ll E_F$, (which is the Migdal's condition for the applicability of Eliashberg theory) since in pnictides E_F is always on the order of 5 eV or more.[20] The experimental temperature dependence of the gaps shown in the upper panel of Fig. 3 is rather unusual, with the gaps slightly decreasing with increasing temperature until they suddenly drop close to T_c. The theory reproduces very well this behavior, which is possible only in a very strong-coupling regime.[16] The different temperature dependence observed in the lower panel of Fig. 3 results from a complex nonlinear dependence of Δ_i vs T curves on λ_{31}. Further details will be given in a forthcoming paper. It is worth noticing that the absolute values of the large gaps *cannot* be reproduced in a interband only, two-band Eliashberg model[21] nor within a three-band BCS model. In the latter case it is only possible to obtain a ratio of the gaps close to the experimental one.[8,10]

TABLE I. The effect of a small contribution of intraband coupling, λ_{ii}=0.4 for the case of $Ba_{0.6}K_{0.4}Fe_2As_2$ at T=2 K.

λ_{31}=3.866	λ_{32}=0.471	μ^*_{ij}=0, λ_{ii}=0.4
Δ_1=10.30 meV	Δ_2=5.62 meV	$\lvert\Delta_3\rvert$=10.24 meV

TABLE II. The effect of the Coulomb interaction, μ_{ij}^* for the case shown in Table I.

$\lambda_{31}=2.730$	$\lambda_{32}=0.758$	$\mu_{ij}^*=0.1$, $\lambda_{ii}=0.4$
$\Delta_1=7.49$ meV	$\Delta_2=5.72$ meV	$\lvert\Delta_3\rvert=7.98$ meV

Figure 4 shows the results of such a three-band BCS calculation for $Ba_{0.6}K_{0.4}Fe_2As_2$ (left) and $SmFeAsO_{0.8}F_{0.2}$ (right). Here ω_D has been chosen so as to give the correct T_c (ω_D=7.58 and 15.00 meV, respectively) and the coupling constants λ_{ij}^{BCS} are the BCS limit of the λ_{ij} used in Fig. 3. It is clear that this model fails in reproducing the gap values and their temperature dependence, leaving the doubt that some additional ingredient could be necessary to obtain a quantitative agreement with experiments. As shown above, this is not the case in the Eliashberg approach.

In this regard, we also tested the effect into the model of a small intraband coupling (possibly of phonon origin). In $Ba_{0.6}K_{0.4}Fe_2As_2$ we used $\lambda_{ii}=0.4$ since we know indeed that this coupling cannot be very high.[5] Contrary to naïve expectations, this term does not sensibly increase the gap values. In fact, as it can be seen in Table I, the gap values only show a slight increase (of about 1%).

The effect of Coulomb interaction was also investigated for the case shown in Table I where a weak intraband coupling is included. We chose $\mu_{ij}^*=0.1$ and, as expected, we found that the intraband Coulomb pseudopotential has a negligible effect while the interband one[14] strongly contributes to raise T_c and reduces in a considerable way the value of λ_{31}: in this case, as shown in Table II, it is only possible to obtain the correct value of the small gap. This result seems thus to exclude a strong interband Coulomb interaction in these compounds.

Finally we have also examined, for $SmFeAsO_{0.8}F_{0.2}$, the case of a spectral function with two peaks at energies Ω_1 and Ω_2. In Fig. 5 the two boson energies are $\Omega_1=10$ meV and $\Omega_2=20$ meV. The gap values (left axis) and the coupling constants, λ_{31} and λ_{32} (right axis) are plotted as a function of the weight of the low-energy peak, w_p. As somehow expected, when the weight of this peak increases, the gaps Δ_1 and $|\Delta_3|$ increase (and approach the experimental ones) but also the coupling constants, λ_{31} and λ_{32} strongly increase. A similar behavior can be observed if $\Omega_1=10$ meV and $\Omega_2=30$ meV, although the gaps Δ_1 and $|\Delta_3|$ are smaller.

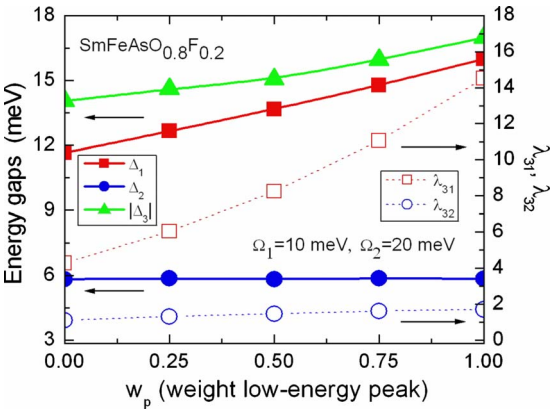

FIG. 5. (Color online) The calculated gaps and electron-boson coupling constants λ_{31} and λ_{32} in the 1111 case as function of the weight w_p of the low-energy peak $\Omega_1=10$ meV. Here $\Omega_2=20$ meV.

In conclusion, we have shown that the recently discovered iron pnictides are very likely to represent an example of dominant negative interband-channel pairing superconductivity where an electron-boson coupling, such as the electron-SF one, can become a fundamental ingredient to increase T_c in a multiband strong-coupling picture. In particular, the present results first prove that a simple three-band model in strong-coupling regime can simultaneously reproduce in a quantitative way the experimental T_c *and* the energy gaps of the pnictide superconductors with only two free parameters, λ_{31} and λ_{32}, provided that the typical energies of the spectral functions are on the order of 10 meV and the coupling constants are very high ($\lambda_{31}>4$).

We thank I. I. Mazin and E. Cappelluti for useful discussions.

*giovanni.ummarino@infm.polito.it

[1] Y. Kamihara *et al.*, J. Am. Chem. Soc. **130**, 3296 (2008).
[2] Z. A. Ren *et al.*, Chin. Phys. Lett. **25**, 2215 (2008).
[3] M. Rotter, M. Tegel, and D. Johrendt, Phys. Rev. Lett. **101**, 107006 (2008).
[4] C. de la Cruz *et al.*, Nature (London) **453**, 899 (2008).
[5] L. Boeri, O. V. Dolgov, and A. A. Golubov, Phys. Rev. Lett. **101**, 026403 (2008); Physica C **469**, 628 (2009).
[6] I. I. Mazin, D. J. Singh, M. D. Johannes, and M. H. Du, Phys. Rev. Lett. **101**, 057003 (2008).
[7] Physica C 469, (2009), special issue on pnictides.
[8] L. Benfatto, M. Capone, S. Caprara, C. Castellani, and C. Di-Castro, Phys. Rev. B **78**, 140502(R) (2008).
[9] I. I. Mazin and J. Schmalian, Physica C **469**, 614 (2009).
[10] E. Z. Kuchinskii and M. V. Sadovskii, JETP Lett. **89**, 156 (2009).
[11] G. M. Eliashberg, Sov. Phys. JETP **11**, 696 (1960).
[12] H. Ding *et al.*, EPL **83**, 47001 (2008).
[13] D. Daghero, M. Tortello, R. Gonnelli, V. Stepanov, N. Zhigadlo, and J. Karpinski, Phys. Rev. B **80**, 060502(R) (2009).; R. S. Gonnelli *et al.*, Physica C **469**, 512 (2009).
[14] G. A. Ummarino, J. Supercond. Novel Magn. **20**, 639 (2007).
[15] E. J. Nicol and J. P. Carbotte, Phys. Rev. B **71**, 054501 (2005); G. A. Ummarino *et al.*, Physica C **407**, 121 (2004).
[16] G. A. Ummarino and R. S. Gonnelli, Physica C **328**, 189 (1999).
[17] A. D. Christianson *et al.*, Nature (London) **456**, 930 (2008); R. Osborn *et al.*, Physica C **469**, 498 (2009).
[18] G. Varelogiannis, Physica C **249**, 87 (1995)
[19] I. I. Mazin, private communication.
[20] A. S. Sefat, R. Jin, M. A. McGuire, B. C. Sales, D. J. Singh, and D. Mandrus, Phys. Rev. Lett. **101**, 117004 (2008); I. A. Nekrasov, Z. V. Pchelkina, and M. V. Sadovskii, JETP Lett. **87**, 560 (2008); and **88**, 144 (2008).
[21] O. V. Dolgov, I. I. Mazin, D. Parker, and A. A. Golubov, Phys. Rev. B **79**, 060502(R) (2009); G. A. Ummarino, J. Supercond. Novel Magn. **22**, 603 (2009).